# AERODYNAMIC STUDY OF A NOVEL TRAILING-EDGE FLAP CONCEPT OF A HIGH-LIFT TRANSPORT CONFIGURATION

**Wojciech Kania*, Włodzimierz Gnarowski*, Wieńczysław Stalewski***
**Simon Galpin**, Zdobysław Goraj***, Marcin Figat*****

***Institute of Aviation, Warsaw, Poland**
****Airbus UK, Filton, United Kingdom**
*****Warsaw University of Technology, Warsaw, Poland**

**Keywords**: *aerodynamics, high-lift technology, CFD, adaptive elements, HELIX*

## Abstract

*A development of a novel, highly aerodynamically efficient high-lift system for future transport aircraft is one of today's challenges. HELIX – the project under the V FR Programme of EU – aims to explore new ideas concepts put forward by the participating companies and research institutions by gaining on their vast experiences and expertise in the field of high-lift aerodynamics and systems and putting these to best advantage. One of as many as 21 different concepts considered within HELIX project is the so-called "Segmented Extension Slotted Flap" (SESF). The SESF uses a novel flap mechanism completely embedded in the wing structure. It allows to remove the flap track fairings, what eliminates the unfavorable impact of the high-lift system on the cruise drag. The SESF concept consists of an autonomous segmented trailing edge along all wing span. The outer segment acts as flaperon. Each flap segment is composed of two elements: movable fore box, which forms a slot at take-off and landing and movable main flap.*
*Weight analysis indicates that the SESF deployment mechanism is considerably lighter than for a classical Fowler type flap. For analyzing of the cruise and high-lift configuration the 3-D surface panel method coupled with boundary layer and the Euler code on the unstructured grids were used. Results from panel code obtained in WUT (VSAERO software) and from Euler code (obtained in Airbus UK) were used in the design optimization process.*

## 1 Introduction

In recent years, the demand for a cheaper, more efficient but of lower environmental impact and easy to maintain aircraft has led designers and manufacturers alike to respond resolutely with the introduction of aircraft closely matching these requirements, for example A330/340, A380, B777 and B7E7. One important area that has made a significant contribution to these goals is high-lift technology. High-lift systems for civil transport aircraft are generally complicated and they induce complex physical flow phenomena.

A development of a novel, highly aerodynamically efficient high-lift system for future transport aircraft is one of today's challenges advanced by European GoP in [1]. Improved high-lift performance will lead to more safety transport aircraft and of lower operating cost. It will allow to reduce the noise at take-off and landing. Due to increase of lift to drag ratio and a reduction of weight of high-lift system, it is possible to reduce the fuel burn, causing environmental benefits near airports as well as in global scale.

It is also possible to use a novel high-lift system as a wing adaptive element to optimize a wing shape to an actual cruise condition [2-5]. Application of such adaptive wing may results in a reduction of direct operating cost (DOC).

Within the HELIX project (Innovative Aerodynamic High-Lift Concepts) supported by the European Commission, Institute of Aviation has developed the novel high-lift system concept. This system was named Segmented Extension Slotted Flap (SESF).

## 2 Short description of the HELIX project

The development of the SESF high-lift system has been conducted within the HELIX (Innovative High-Lift Aerodynamic Concepts) project supported by the European Commission in Fifth Framework Programme. Thirteen partners take part in the project coordinated by Airbus UK.

HELIX aims to develop and explore innovative high-lift concepts to overcome the basic problem of providing sufficient (in terms of aerodynamic and noise characteristics), cost effective low speed performance. Within the HELIX project the 21 concepts put forward by the partners have been regularly assessed and compared to a state-of-the art of 200 – 250 seat type aircraft configuration (HELIX baseline aircraft) with a traditional high-lift system (single slotted slats and flaps) for a range of representative missions.

The data determined by the partners for each concept have been analyzed using the multidisciplinary trade tools by the industrial partners: Airbus UK and IAI, in four design cycles during the first year of the project. The results of the multi-disciplinary trade analysis have been used to down select the six best concepts at the end of the first year of the project. This down selection process was based upon three possible customer-driven requirements, namely:

- higher performance at the same cost
- the same performance at lower cost
- lower environmental impact at the same cost.

The process of maturity and trade-off analysis of the selected concepts has been continued during the second year of the project. The best one concept has been down selected at the end of the second year of the project. The concept will be extensively validated in large-scale experimental low and high Reynolds number tunnel tests during the last year of the project.

More details about the HELIX project can be found in [6].

## 3 Segmented Extension Slotted Flap (SESF) high-lift system

### 3.1 The idea of the SESF concept

The concept of the Segmented Extension Slotted Flap high-lift system is based on the conventional HELIX baseline slat and developed a novel segmented trailing edge flap which can be extended and deflected. It is an all–span trailing flap consisted of four autonomous flap segments, as it is shown in Fig. 1, with outer segment acting as flaperon. The main beneficial feature of the SESF concept is a novel flap deployment mechanism, which is entirely embedded within a contour of the wing. This mechanism is simpler and lighter than that of the Fowler type flap, usually used in conventional high-lift systems for civil transport aircraft. The SESF high-lift system allows to remove the flap track fairings, what eliminates the unfavorable impact of a high-lift system on the high speed/cruise wing shape, thereby reducing the wing drag at these flight conditions. Figure 3 shows comparison of the deployment mechanism of the SESF concept and generally used conventional Fowler type.

Each flap segment is composed of two elements: movable fore box, which forms a slot at take-off and landing as it is shown in Fig. 2 and movable main flap with thickness ratio greater than the Fowler flap applied in HELIX baseline high-lift system. Both elements have built-in rollers and move in tracks, driven by an autonomous hydraulic driving mechanism. For

each flap segment an autonomous hydraulic drive mechanism is fastened to a rear wing spar.

Additional feature of the SESF high-lift system is a capability of the flap deflection up to 5 deg. realized without gap (see Fig. 2a and 2b) what allows to optimize the wing camber to the actual cruise lift coefficient changeable due to weight losses through burning fuel. Due to a large curvature radius of the flap tracks, the SESF concept maintains the smooth upper wing surface for gapless deflected configuration required to reduce intensity of a shock wave at cruise.

### 3.2 Aerodynamic design of the SESF high-lift system

Development process of the SESF high-lift system was based on the 2D and 3D HELIX Baseline three-element models [7]. The Fowler type flaps used in these models were replaced by new design novel SESF flaps described above. The main constraints in design of the SESF system were:

- shape of the wing with SESF high-lift system in nested configuration must be just like the HELIX Baseline wing
- the rear spar must be in the same position like in HELIX baseline.

In realizing the numerical design of the 2D HELIX SESF trailing edge device several CFD were used:

- MSES [8] – two dimensional analysis and design code for multi-element airfoil based on the viscous-coupled Euler method with simulation of the flow separation
- CODA [9] – multi-element two-dimensional analysis and design code based on the panel method
- HCZMAX [10] – airfoil analysis code based on the viscous-coupled potential method with simulation of the separated region effects.

At first step initial geometry of the SESF high-lift devices (fore box and main flap) fulfilling constraints was determined. Afterward initial version of the 2D SESF device was designed using above CFD codes. Taking the initially designed 2D SESF device as base airfoil for wing geometry the first three-dimensional (3D) model of HELIX wing with the SESF device (HELIX SESF wing) was designed.

A three-dimensional numerical study of the high-lift performance of the 3D HELIX Baseline and 3D HELIX SESF models at landing was performed using FLITE 3D code based on Euler method [11].

The numerical results for the 3D HELIX SESF model are quite promising but $C_{Lmax}$ is lower than for Baseline model [11]. In next step two-dimensional numerical optimization was undertaken to improve high-lift performance of the SESF trailing edge device, especially $C_{Lmax}$ at landing and lift to drag ratio at take-off. The two-element 2D Baseline and SESF models (with slat retracted for simplification) were studied for the fore box and flap optimization. Various flap and fore box deflections and positions have not been resulted in satisfactory improvement of $C_{Lmax}$ at landing. The flap was redesigned to decrease pressure gradient over the flap upper surface at landing, as it is shown in Fig. 5. After several modifications 2D SESFws16 model was designed. It features some improvement of $C_{Lmax}$ at landing in comparison to initial version and higher $C_{Lmax}$ by 4% and lift to drag ratio by 8% at take-off condition than baseline model. The high lift performance of 2D SESFws16 model in comparison with 2D Helix baseline model at take-off are shown in Fig. 6 and 7.

To improve $C_{Lmax}$ at landing of the 2D SESFws16 model, the flap performance for two-element SESF model was optimized by numerical calculation using viscous MSES code at various gap and overlap settings. By moving the main flap through a grid of 25 points, the maximum lift coefficient was improved as it is shown in Fig. 8. The aerodynamic coefficients for the optimized flap position of 2D HELIX SESFws16 are compared to the 2D HELIX baseline at landing configuration in Fig. 9.

### 3.3 The flap deployment mechanism and weight evaluation

For each segment of the trailing edge of SESF high-lift system an autonomous hydraulic deployment mechanism is fastened to the rear wing spar. The deployment mechanism consists of three main sub-assemblies:

- hydraulic motor
- gear
- self-locking ball screw.

The deployment mechanism of the inboard SESF lift-high device segment, realizing cylindrical movement, is outlined in Fig. 4. For the outboard segments, in order to realize conical movement, the outlined deployment mechanism was modified. Modification principally concerned of the replacement of the screw actuators (elements 6 and 7 – see Fig. 4) located along the rear spar by the screw actuators set streamwise and fastened through Cardan joints to the rear spar. Moreover, the spring actuators on ball-and-socket joints were mounted to the structure of the fore box.

Approximately 500 repeatable elements of the SESF high-lift system were specified. Based on this specification and on the HELIX baseline aircraft weight breakdown [12], the weight saving for the SESF system was evaluated. It was concluded that weight saving for structure and deployment mechanism is approximately 500 kg, what makes about 35% of the trailing edge total weight of the HELIX baseline wing.

The SESF concept has been investigated by QinetiQ in order to provide a detailed assessment of the weight and structural high-lift system [15]. A detailed three-dimensional solid model assembly of the SESF inboard segment was constructed using the Unigraphics NX. It was concluded that the SESF model is fully constrained to control the position and displacements of all actual components. QinetiQ weight assessment also revealed the SESF concept weight saving [14, 15].

More details of the SESF deployment mechanism, including weight saving evaluation, are presented in [13-15].

## 4 Three-dimensional numerical analysis of the aerodynamics of the SESF high-lift system

Design of the 3D HELIX SESF wing model was based on the 2D HELIX SESFws16 three-element airfoil, presented in chapter 3.2, with optimized the overlap and gap at landing configuration. At four sections of the wing: root, kink, flap extent and tip, the above mentioned basic airfoil was redesigned according to geometrical parameters of the HELIX wing model. Two-element airfoils (slat retracted for simplification) at above mentioned sections of HELIX baseline and HELIX SESF wings have been calculated using MSES code. The high-lift performance benefits of the HELIX SESF two-element airfoils relative to the HELIX baseline are approximately the same like 2D basic HELIX SESFws16 and HELIX baseline models mentioned in chapter 3.2.

The geometry of both 3D models: HELIX baseline [7, 12] and HELIX SESF wings at cruise configuration are the same. At take-off and landing configurations both models differ only in trailing edge high-lift devices.

Three-dimensional CFD numerical analysis of the high-lift performance for the both models: 3D HELIX baseline and 3D HELIX SESF at take-off and landing configurations have been conducted. Two different CFD codes were used: FLITE 3D and VSAERO.

The slat deflections $\delta_s$ were the same for both models:

- at take-off $\delta_s=23$ *deg*.,
- at landing $\delta_s=27$ *deg*.

The flap deflection were different for these models:

- for baseline $\delta_f=22.3$ deg. at take-off and $\delta_f=35$ deg. at landing
- for SESF $\delta_s=22$ *deg*. at take-off and $\delta_f=30$ *deg*. at landing.

Results of the 3D HELIX SESF and baseline models of high-lift performance, calculated using FLITE 3D code are compared in Fig. 10 and 11. At take-off configurations the comparison shows noticeable improvement of high-lift performance due to the SESF high-lift system. The effects of the SESF system are: an

increase in maximum lift coefficient $C_{Lmax}$ by approximately 5% and the drag coefficient reduction (at safe take-off $C_L$) by 160 drag counts. Lift to drag ratio at the take-off $C_{Lto}$ defined as $C_{Lmax}$ $/1.13^2$ for the 3D HELIX SESF model is higher by 7,5% than for Baseline model. The high-lift performance for landing configurations of both models are nearly the same. The maximum lift coefficient for the 3D HELIX SESF model is lower by 0.03 than for baseline model. The further works to improve high-lift performance of the 3D HELIX SESF landing configuration through increase the flap deflection are under way.

The effects of the SESF system on the high-performance of the HELIX model have been confirmed by the results of the both models numerical calculation using VSAERO code [17] (see in Fig. 14). The lift coefficients of the HELIX SESF model at take-off and landing configurations obtained by two computational methods (FLITE 3D and VSAERO) are compared in Fig. 15. An agreement is quite good. Pressure distributions on the wings of the 3D HELIX SESF and baseline models at take-off configuration obtained using VSAERO code are presented in Fig. 16. Comparisons are made at two spanwise sections: $2y/b=0.2$ (inboard wing) and $2y/b=0.55$ (outboard wing). It can be seen that benefits in the lift coefficient are mostly caused by load increase on the main box of the wing.

## 5 Application of the SESF high-lift system to the HELIX aircraft

In order to provide a reliable assessment of the novel high-lift concepts developed within the project the HELIX baseline DOC optimized aircraft has been established [12]. The baseline aircraft is equipped with conventional state-of-the-art slat and flap system.

Two multi-disciplinary 'trade-off' tools have been used to assess all novel high-lift concepts within HELIX project. Transport Aircraft Design Program with Optimization Logic Executive (TADPOLE), developed by Airbus UK, is a computer-based system to optimize the transport aircraft for DOC, fuel burn, MTOW, OWE, etc. Optimized aircraft is defined by a number of variables. In optimized analysis run these variables are parameters that can be changed by the optimizer in order to improve the aircraft. Each HELIX concept was assessed using TADPOLE, comparing the new DOC with baseline slat/flap high-lift system, taking into account the specified mission and required field and flight performance. IAI used a grading tool FET that is enable for quick and 'automatic' procedure for high-lift concept analysis in simplified approach. Several parameters were studied in FET analysis: BFL, $2^{nd}$ segment gradient, take-off distance, approach speed, cruise L/D and DOC.

The 3D aerodynamic data used in optimized TADPOLE analysis was based on the results of the numerical calculation of the 2D HELIX SESFws16 and baseline models, presented above in chapter 3.2. The 3D aerodynamic characteristics were calculated using viscous–inviscid hybrid method based on coupling 2D viscous sectional characteristics with a modified VLM method [14].

The reduction of the cruise drag coefficient by about 1.3% according to the data in [12] due to elimination of the flap track fairing was taken into account in TADPOLE and FET trade analysis.

TADPOLE-optimized simple run revealed that the most important benefits of the SESF high-lift system are reductions of Direct Operating Cost by 3.9% and block fuel burn by 4.7% in the defined mission .

The high-lift performance, obtained in 3D numerical calculation performed by Airbus and presented above in chapter 4, were used in FET trade-off analysis. Two cases of the take-off were studied: at baseline $C_{Lto}$ and at improved $C_{Lto}$ considering $\Delta C_{Lmax}$ due to the SESF high-lift system. FET results show improvement at take-off: BFL decreases on 2.5% or 4.5%, take-off distance decreases on 1% or 4.4% and second segment gradient increases on 11.7% or 9%, respectively to the baseline $C_{Lto}$ or improved $C_{Lto}$ cases. Landing distance is nearly the same like for HELIX baseline and approach speed decrease by 2%.

Direct Operating Cost (DOC) in FET analysis was evaluated at nominal 2nd segment and nominal BFL. At nominal 2nd segment the DOC is reduced on 16% or 12.7% according to the baseline $C_{Lto}$ or improved $C_{Lto}$ cases. At nominal BFL case the 2nd segment gradient increases on 7.3% and DOC decreases on 7.3%.

Based on the presented above improvement of the field and flight performance the SESF high-lift system has been down selected to the experimental validation in large-scale, low-speed wind tunnels tests at low and high Reynolds number (at Filton – Airbus UK and Farnborough – QinetiQ).

## 6 Conclusions

The novel Segmented Extension Slotted Flap high-lift system was developed. The main beneficial feature of the SESF system is a novel, simpler and lighter flap mechanism, which is entirely embedded within a wing contour. It allows to remove the conventional flap track fairings, what reduces the cruise coefficient drag by 1.3% in comparison to the aircraft with conventional high-lift system (HELIX baseline). Each autonomous flap segment is composed of movable fore box, which forms a slot at high-lift configurations. The SESF system is capable to deflect flap without gap what allows to optimize the wing camber in a cruise.

3D numerical calculation revealed beneficial effects of the SESF system on the high-lift performance of the baseline aircraft. At take-off the SESF system caused an increase in maximum lift coefficient $C_{Lmax}$ on 5% and take-off drag coefficient reduction on 160 drag counts. Lift to drag ratio at the take-off $C_{Lto}$ increases on 7.5%.

TADPOLE optimized trade analysis revealed that the most benefits of the SESF system are reductions of DOC by 3.9% and block fuel burn by 4.7% in the defined mission. More optimistic results obtained in FET trade analysis – DOC reaches value up to 16%.

## References


[1] European Aeronautics: a vision for 2020. Meeting society needs and winning global leadership. *Report of the Group of Personalities*, Jan., 2001.

[2] Fieldings J P. Design investigation of variable—camber flaps for high-subsonic aircraft, *Proceedings of ICAS 2000 Congress* , Paper 124, pp 1-11, 2000.

[3] Monner H P. Realization of an optimized wing camber by using formvariable flap structures. *Aerospace Sci. Technology*, No. 5, pp 445-455, 2001.

[4] Stanewsky E. Adaptive wing and flow control technology. *Progress in Aerospace Sci*., Vol. 37, No. 7, pp 583-667, 2001.

[5] Green J E. Greener by design - the technology challenge. *Aeronaut. Jour*., No 1056, pp 57-85, 2002.

[6] Galpin S A, Melin T. HELIX: Innovative high-lift aerodynamic concepts, an overview. *Proceedings of KATnet/Garteur High Lift Workshop*, Stockholm, Sweden, 17-19 Sept., 2002.

[7] De Carvalho V. 2D and 3D HELIX baseline models. Technical Memorandum HELIX/TM/AUK/VDC 090701/1, 2001.

[8] Drela M. A users guide to MSES2.7., MIT Computational Aerospace Laboratory, November 1994.

[9] Stalewski W. CODA code for assistance in multi-element airfoil design. *IoA Report No. 136/BA/97/D*, 1997 (in Polish).

[10] Rokicki J, Szydelski M. Numerical analysis of airfoil aerodynamic coefficients with simulation of separation flow effects. *IoA Report No. 23/BA/90/H*, 1990 (in Polish).

[11] Buma S, Galpin S A. 3D evaluation of the high-lift performance on the Segment Slotted Flap concept within the HELIX Programme. *Airbus Technical Report Ref. DMS wind chill 32976*, 2003.

[12] Galpin S A. Description of the baseline DOC optimized aircraft for the HELIX project. *Memo No. HELIX/TM/AUK/SAG090701/6*, pp. 1-12, 2002.

[13] Gnarowski W, Kania w. Segmented extension slotted flap. *Technical Report No. HELIX/TR/IoA/WG-WK/240502/1*, pp. 1-39, 2002.

[14] Gnarowski W, Kania W. Segmented extension slotted flap. *Technical Report No. HELIX/TR/IoA/WG-WK/150803/2*, pp. 1-60, 2003.

[15] Lynn R, Rae A. A weight assessment of the a spanwise fence and segmented extension slotted flap concepts, *Technical Report No. QINETIQ/FST/TR032736*, pp. 1-55, 2003.

[16] Gabillard L, Galpin S A. 3D evaluation of the high-lift performance of the Segmented Slotted Flap concept with new IoA geometry (Model B). *Airbus UK Technical Report, Ref. WC54084*, 2003.

[17] Figat M, Goraj Z, Grabowski T., Aerodynamic analysis of 3D HELIX configurations using VSAERO cod. *IAAM Technical Report No. 1/2003*, 2003 (in Polish).

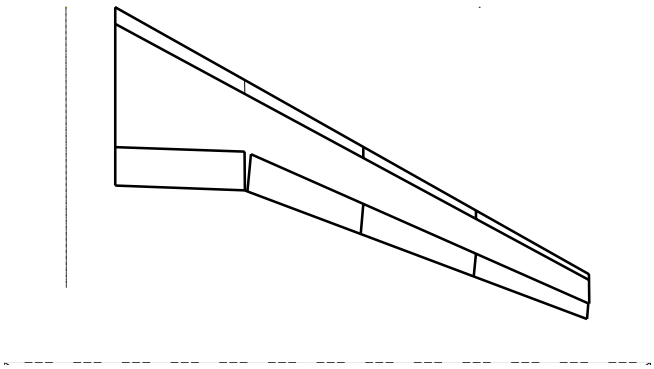

Fig. 1. HELIX Segmented Extension Slotted Flap (SESF) high-lift system.

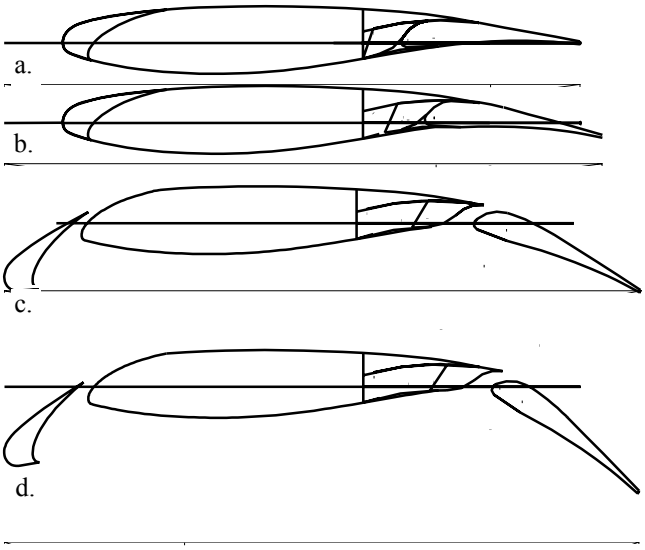


Fig. 2. The cruise (a, b), take-off (c) and landing (d) configurations of the HELIX SESF high-lift system. The cruise configuration is shown with settings for minimum and maximum camber.

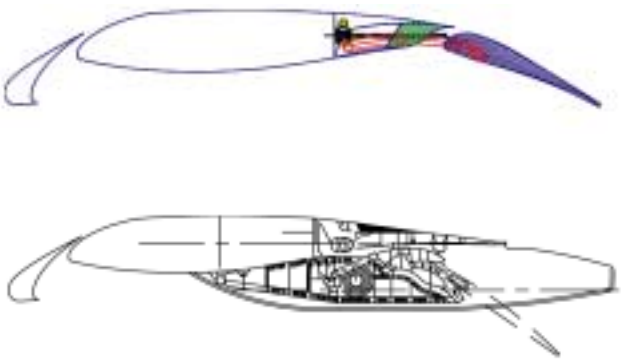

Fig. 3. Comparison of the HELIX SESF high-lift system at landing configuration with generally used Fowler flap deployment mechanism.

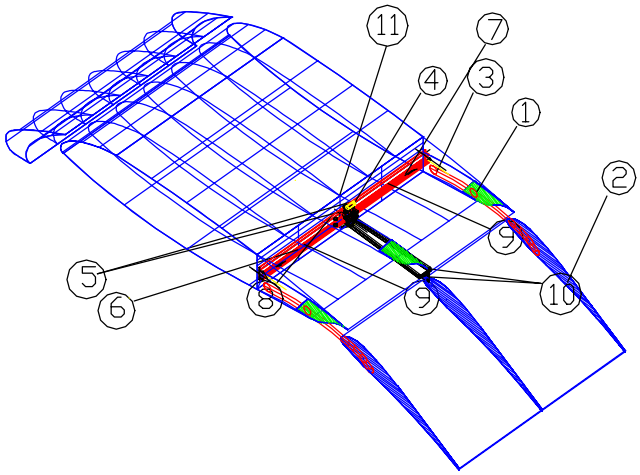


Fig. 4. Inboard wing segment with flap deployment mechanism at landing configuration
1- fore box of the flap; 2- main flap box;
3- flap tracks; 4- gear; 5- hydraulic motors;
6- left screw; 7- right screw; 8- pusher carriage;
9- carriage guide; 10- pushers;
11- plane of the rear spar.

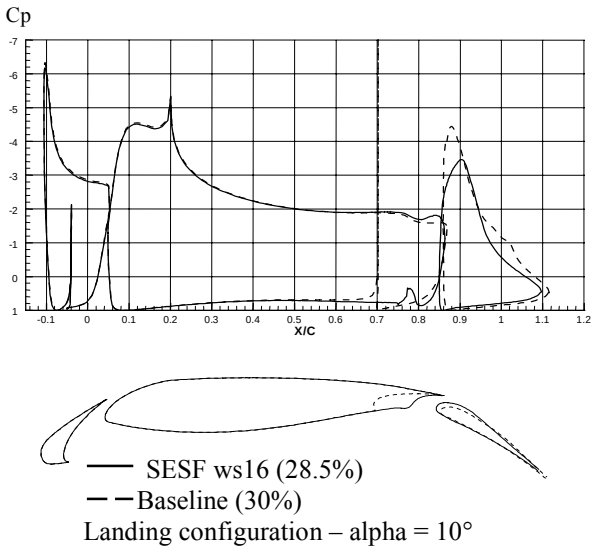


Fig. 5. Comparison of the 2D HELIX SESFws16 and 2D HELIX baseline high-lift system models at landing configuration. Pressure distribution at angle of attack 10 deg. MSES code

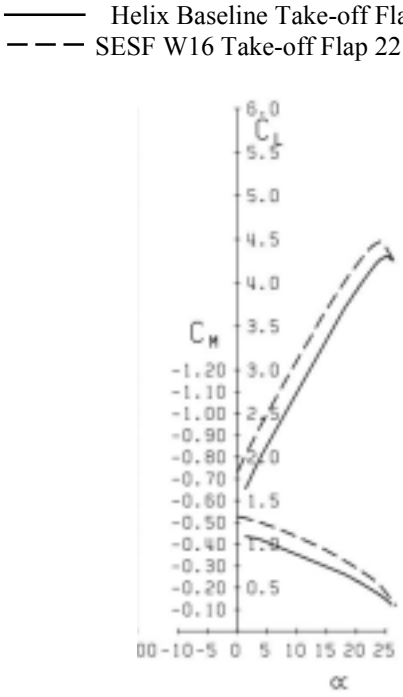


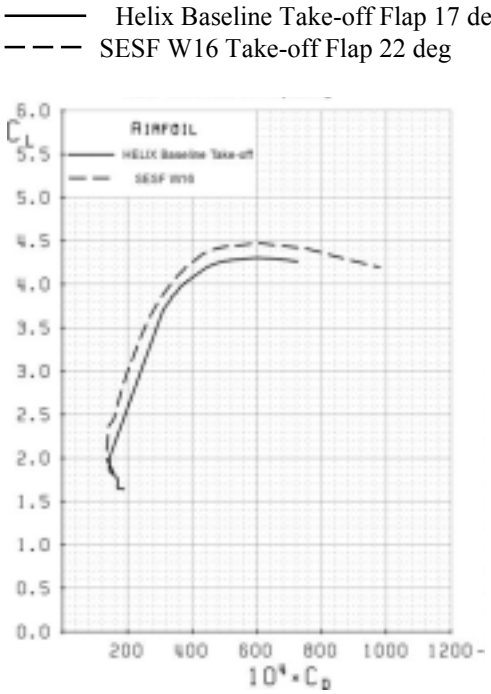


Fig. 6. Comparison of the aerodynamic coefficients for the three-element 2D HELIX SESF and 2D HELIX baseline models at take-off. MSES code (Mach number M=0.2, Reynolds number Re=6∗10$^6$)

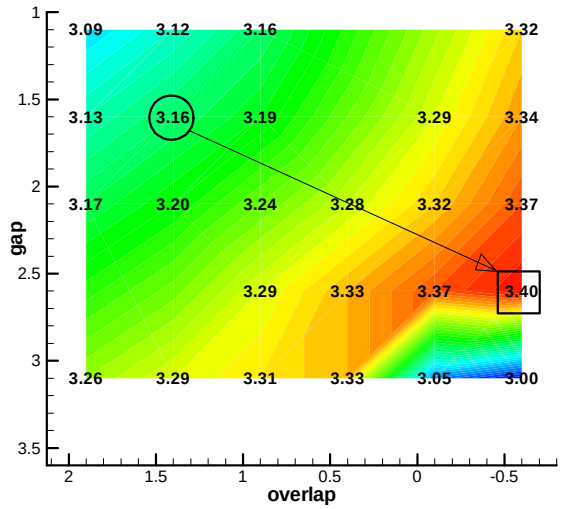


Fig. 7. The flap overlap and gap optimisation for the two-element 2D HELIX SESF model at landing ($\delta_f$=30°). (Mach number M=0.2, Reynolds number Re=6∗10$^6$), MSES code, O – initial flap position

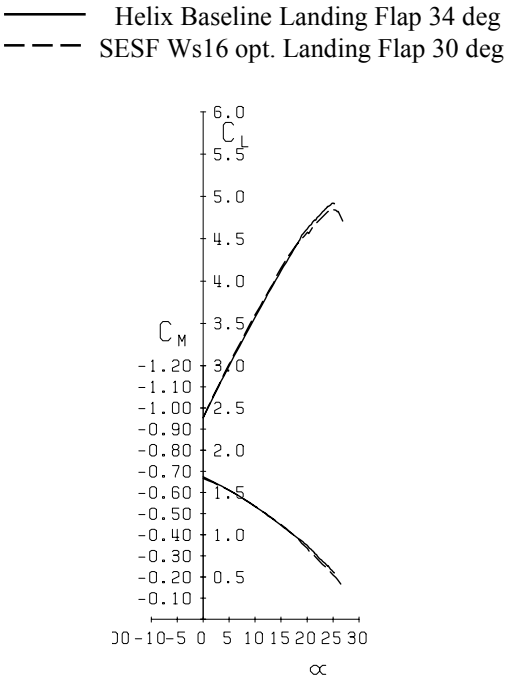


Fig. 8. Comparison of the lift and pitching moment coefficients for the three-element 2D HELIX SESF (optimized flap position) and 2D HELIX baseline model at landing. MSES code.
(Mach number M=0.2, Reynolds number Re=6∗10$^6$)

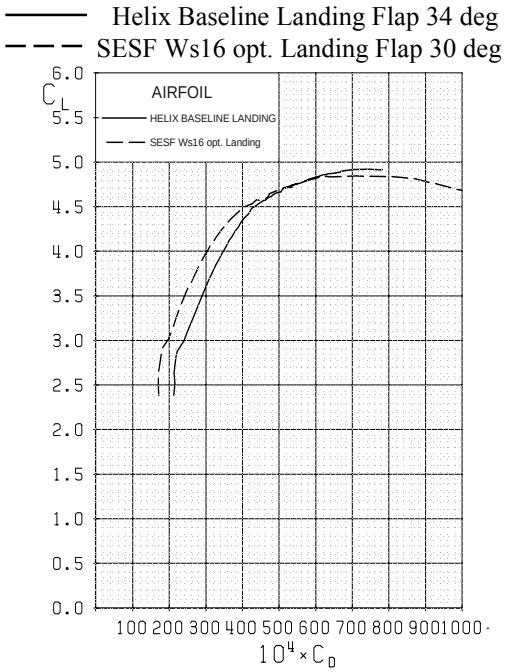


Fig. 9. Comparison of the drag polars for the three-element 2D HELIX SESF (optimized flap position) and 2D HELIX baseline model at landing. (Mach number M=0.2, Reynolds number Re=6∗10$^6$)

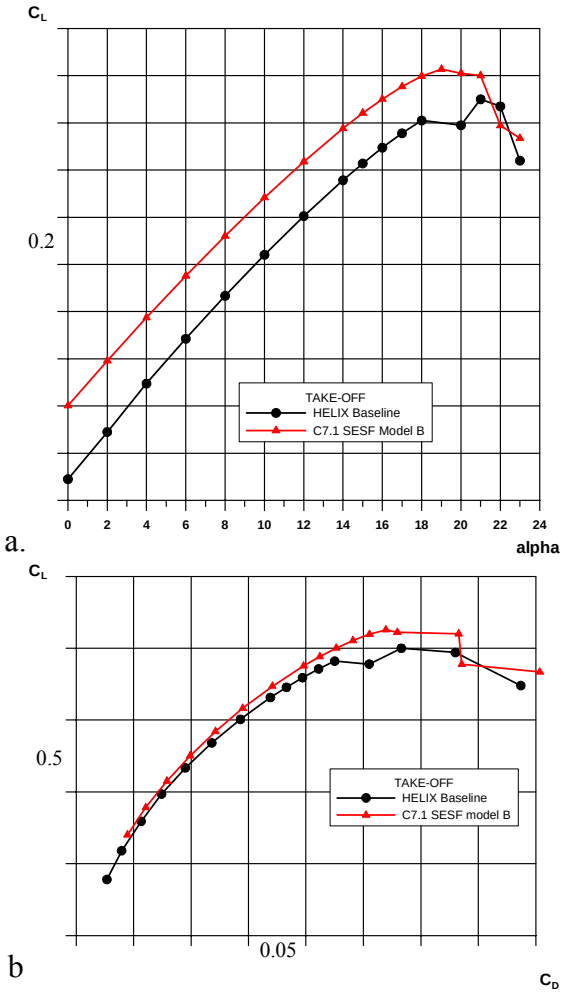


b.

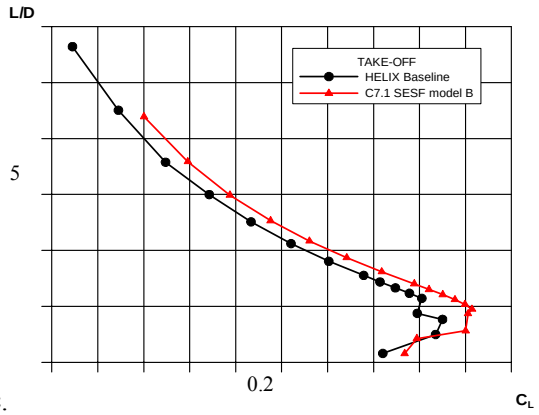


c.

Fig. 10. Comparison the lift and drag coefficients and lift to drag ratio for 3D HELIX SESF and 3D HELIX baseline models (wing/configuration) at take-off. FLITE 3D code [20].

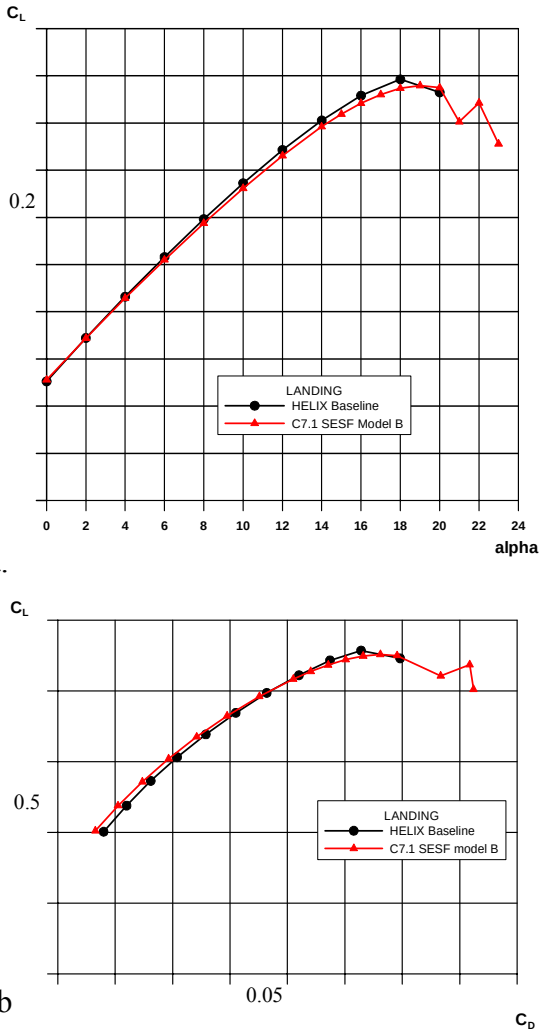


Fig. 11. Comparison the lift and drag coefficients for 3D HELIX SESF and 3D HELIX baseline models (wing/body configuration) at landing. FLITE 3D code [20].

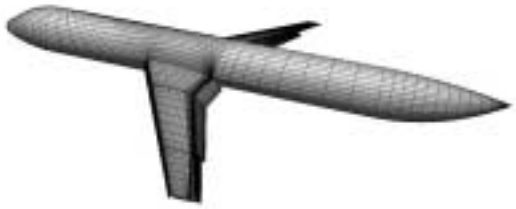

Fig. 12. 3D HELIX baseline model.

Fig. 13. 3D HELIX SESF model.

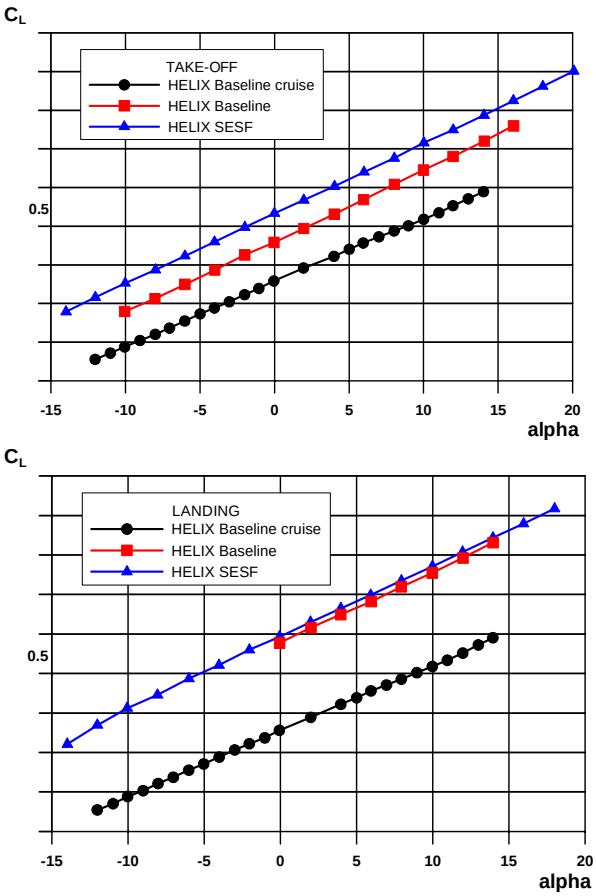


Fig. 14. Comparison of the lift coefficients for 3D HELIX SESF and 3D HELIX baseline models (wing/body configuration) at take-off and landing (M=0.2, Re=21.4∗10$^6$). VSAERO code [21].

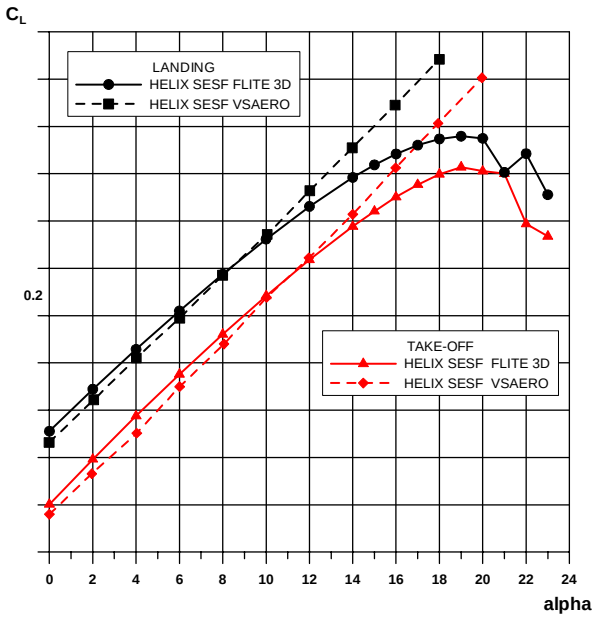


Fig. 15. Comparison of the lift coefficients of the 3D HELIX SESF model at take-off and landing configurations calculated by FLITE 3D and VSAERO codes.

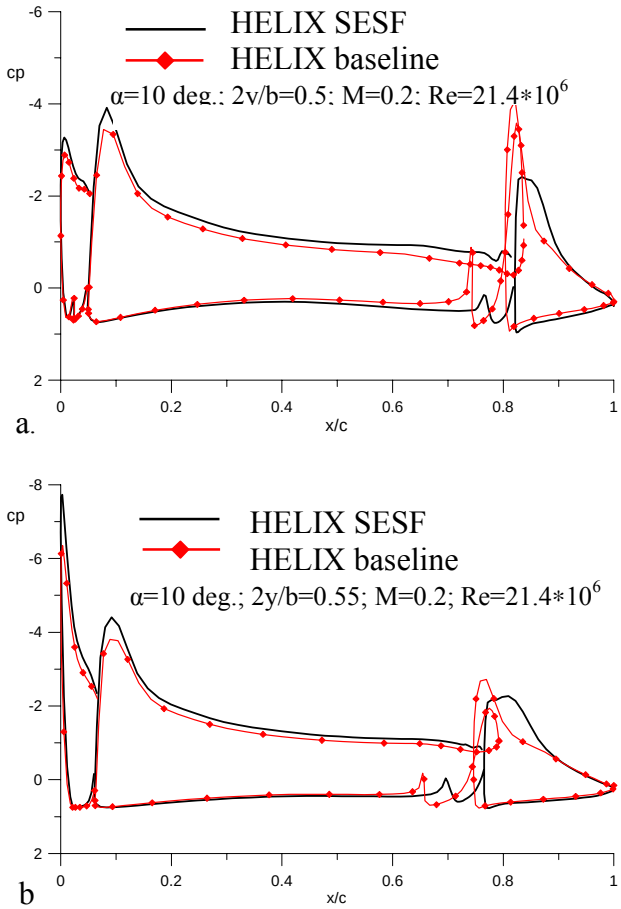


Fig. 16. Comparison of the pressure distributions on the wings of the 3D HELIX SESF and baseline models. VSAERO code.